

Static Properties of the Multiple-Sine-Gordon Systems

M. Peyravi¹, N. Riazi^{1*} and Afshin Montakhab^{2†}

1. *Physics Department and Biruni Observatory, Shiraz University, Shiraz 71454, Iran,*

2. *Physics Department, Shiraz University, Shiraz 71454, Iran.*

In this paper, we examine some basic properties of the multiple-Sine-Gordon (MSG) systems, which constitute a generalization of the celebrated sine-Gordon (SG) system. We start by showing how MSG systems can be viewed as a general class of periodic functions. Next, periodic and step-like solutions of these systems are discussed in some details. In particular, we study the static properties of such systems by considering slope and phase diagrams. We also use concepts like energy density and pressure to characterize and distinguish such solutions. We interpret these solutions as an interacting many body system, in which kinks and antikinks behave as extended particles. Finally, we provide a linear stability analysis of periodic solutions which indicates short wavelength solutions to be stable.

PACS: 05.45.Yv, 05.00.00, 02.60.Lj, 24.10.Jv

I. INTRODUCTION

The double-Sine-Gordon (DSG) equation which is a generalization of the ordinary Sine-Gordon (SG) equation has been the focus of much recent investigations [1–15]. It has been shown to model a variety of systems in condensed matter, quantum optics, and particle physics [2]. Condensed matter applications include the spin dynamics of superfluid ^3He [3, 4], magnetic chains [5], commensurate-incommensurate phase transitions [6], surface structural reconstructions [7], and domain walls [8, 9] and fluxon dynamics in Josephson junction [10].

In quantum field theory and quantum optics, DSG applications include quark confinement [11] and self-induced transparency [12]. The internal dynamics of multiple and single DSG soliton configurations using molecular dynamics have been studied in [2]. There have also been studies about kink anti-kink collision processes for DSG equation [13]. One can also point to the statistical mechanics applications [14], and perturbation theory for this system [15]. Following our previous study on the periodic and step-like solutions of DSG equation [1], we focus on a generalization of this system with the self-interaction potential (see Fig.1)

* email: riazi@physics.susc.ac.ir

† email: montakhab@shirazu.ac.ir

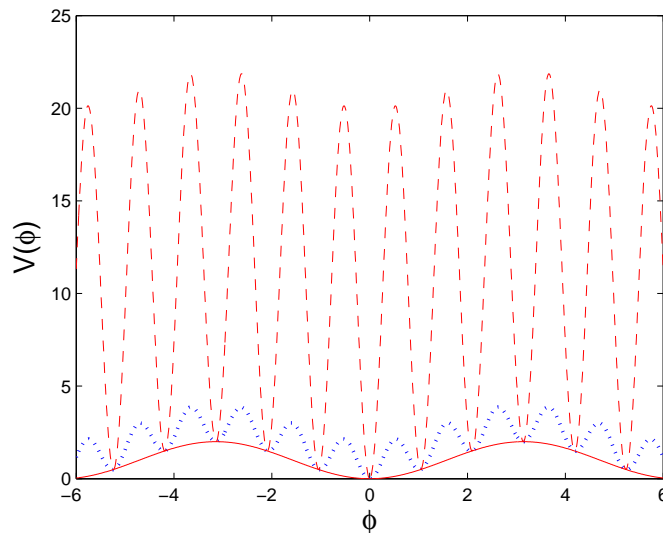


FIG. 1: MSG Potential for $N = 6$. The dashed curve is for $\epsilon = 10$, the dotted curve is for $\epsilon = 1$ and the solid curve is for $\epsilon = 0$.

$$V(\phi) = 1 + \epsilon - \cos \phi - \epsilon \cos(N\phi), \quad (1)$$

where ϵ is a non-negative constant. This potential reduces to the ordinary SG potential in the limit $\epsilon \rightarrow 0$. N is an integer with $N = 1$ and $N = 2$ corresponding to the SG and DSG systems, respectively [1, 16]. In this paper, we propose to study this system along the line of our previous work on DSG [1] for $N > 2$. In Section II we present some general properties of the system including the single kink solutions, in Section III we examine the $N = 3$ case, in Section IV, $N \geq 4$ cases are discussed, and in Section V the stability of periodic solutions is examined. Section VI is devoted to a summary and conclusions.

II. GENERAL PROPERTIES OF THE MSG SYSTEM

The Lagrangian density of the Multiple-Sine-Gordon (MSG) system is the following:

$$\mathcal{L}_{MSG} = \frac{1}{2} \partial^\mu \phi \partial_\mu \phi - [1 + \epsilon - \cos \phi - \epsilon \cos(N\phi)]. \quad (2)$$

From this Lagrangian density, the MSG equation follows

$$\square \phi = -\sin \phi - N\epsilon \sin(N\phi). \quad (3)$$

Note that ϕ is a real scalar field, and we are using a 1+1 dimensional spacetime (t,x) with the signature (+,-). The potential for this system has minima at

$$\phi_{min} = 2n\pi \quad n = 0, 1, 2, \dots \quad (4)$$

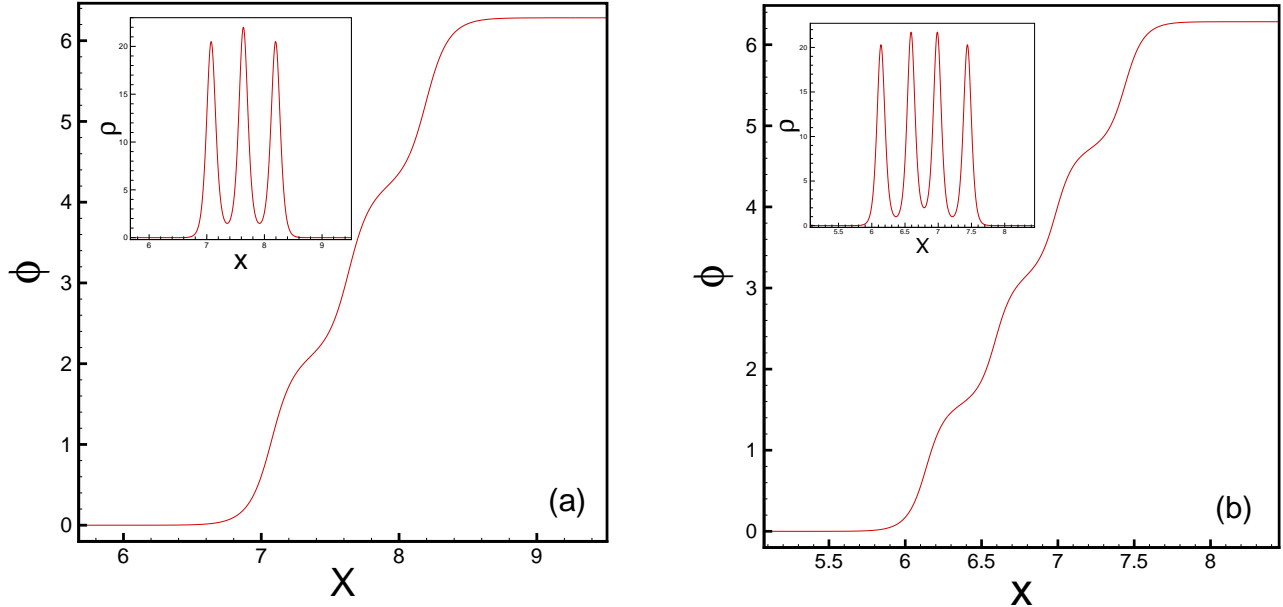


FIG. 2: Single soliton solutions and energy densities (inset) of the MSG system for (a) $N = 3$, $\epsilon = 10$ and (b) $N = 4$, $\epsilon = 10$.

The energy-momentum tensor of the MSG equation can be obtained by the standard relation which follows from the Noether's theorem and is a consequence of the translational invariance of the Lagrangian density:

$$T^{\mu\nu} = \partial^\mu \phi \partial^\nu \phi - g^{\mu\nu} \mathcal{L}_{MSG}, \quad (5)$$

in which $g^{\mu\nu} = \text{diag}(1, -1)$ is the metric of the Minkowski spacetime.

Like the ordinary SG system, a topological current can also be defined for the MSG system according to

$$J^\mu = \frac{1}{2\pi} \epsilon^{\mu\nu} \partial_\nu \phi, \quad (6)$$

where $\epsilon^{\mu\nu}$ is the totally antisymmetric tensor with $\epsilon^{01} = 1$. This current is identically conserved ($\partial_\mu J^\mu = 0$) and the total charge of any localized, finite-energy solution is both conserved and quantized.

MSG equation possesses kink and anti-kink solutions which correspond to transitions between the spatial boundary conditions $\phi(\pm\infty) = 2n\pi$. The first integral of equation (3) for static solutions reads

$$\frac{1}{2} \left(\frac{d\phi}{dx} \right)^2 = V(\phi), \quad (7)$$

in which we have used the boundary conditions $\phi(\pm\infty) = 2n\pi$. We therefore have

$$x - x_0 = \int \frac{d\phi}{\sqrt{2V(\phi)}}. \quad (8)$$

This integral cannot be carried out analytically for general N and ϵ . A few examples of these solutions for $N = 3$ and $N = 4$ which are obtained numerically are shown in Fig.2, together with their energy density, which is equal to the T_0^0 component of T_ν^μ .

Multiple Sine-Gordon systems admit soliton-like kink solutions with interesting properties. Here, we show that an arbitrary, periodic potential with vanishing minima at $\phi = 0$ and $\phi = 2\pi$ can be expanded in terms of MSG potentials. This property adds to our motivation for studying this class of nonlinear equations.

Let us define the MSG basis functions

$$F_N^\epsilon(\phi) \equiv 1 + \epsilon - \cos \phi - \epsilon \cos(N\phi). \quad (9)$$

An arbitrary, periodic function $f(\phi)$ which satisfies the boundary conditions $f(0) = f(2\pi) = 0$ can be expanded in terms of this basis:

$$f(\phi) = \sum_{N=0}^{\infty} a_N F_N^\epsilon(\phi) = (1 + \epsilon) \sum_{N=0}^{\infty} a_N - \cos \phi \left(\sum_{N=0}^{\infty} a_N \right) - \epsilon \sum_{N=0}^{\infty} a_N \cos(N\phi), \quad (10)$$

in which a_N 's are the expansion coefficients. At the same time, $f(\phi)$ can also be represented by a cosine Fourier series:

$$f(\phi) = \sum_{N=0}^{\infty} b_N \cos(N\phi). \quad (11)$$

of course, $f(0) = f(2\pi) = 0$ demands that $\sum_{N=0}^{\infty} b_N = 0$.

Equating the coefficients of $\cos(N\phi)$ in (10) and (11) leads to

$$\begin{aligned} b_0 &= (1 + \epsilon) \sum_{N=0}^{\infty} a_N - \epsilon a_0, \\ b_1 &= - \sum_{N=0}^{\infty} a_N - \epsilon a_1, \\ b_N &= -\epsilon a_N \quad (N > 1). \end{aligned} \quad (12)$$

Note that $\sum_{N=0}^{\infty} a_N$ can be easily calculated via

$$\sum_{N=0}^{\infty} a_N = \frac{1}{2\pi(1 + \epsilon)} \int_0^{2\pi} f(\phi) d\phi. \quad (13)$$

As an example, consider the triangular periodic function

$$f(\phi) = \begin{cases} \phi & 0 \leq \phi \leq \pi \\ 2\pi - \phi & \pi \leq \phi \leq 2\pi \end{cases}$$

with $f(\phi + 2n\pi) = f(\phi)$. The Fourier cosine series representing this function reads

$$f(\phi) = \pi - \frac{8}{\pi} \cos(\phi) - \frac{8}{9\pi} \cos(3\phi) - \frac{1}{4\pi} \cos(4\phi) - \dots \quad (14)$$

The coefficients a_N can be easily calculated from Equations (12) and (13):

$$\begin{aligned} \sum_{N=0}^{\infty} a_N &= \frac{\pi}{2(1+\epsilon)}, \\ a_0 &= -\frac{\pi}{2\epsilon}, \\ a_1 &= \frac{16(1+\epsilon) - \pi^2}{2\pi\epsilon(1+\epsilon)}, \\ a_2 &= 0, \\ a_3 &= \frac{8}{9\pi\epsilon}, \\ a_4 &= \frac{1}{4\pi\epsilon}, \\ &\dots\text{etc} \end{aligned} \quad (15)$$

The reader may get worried about the $\frac{1}{\epsilon}$ dependence as $\epsilon \rightarrow \infty$, but this is not a serious problem, since this is a common factor for all a_N 's and may be factored out.

III. MSG FOR $N = 3$

In this and the next two sections, we investigate some general properties of MSG for $N = 3$, and subsequently for $N = 4$ and $N > 4$, along the line of our previous work on DSG[1]. We focus on the static, time-independent solution of MSG equation. To solve this equation, we use a fourth order Runge-Kutta method[17] to numerically integrate:

$$\frac{d^2\phi}{dx^2} = \frac{dV(\phi)}{d\phi} = \sin\phi + N\epsilon \sin(N\phi). \quad (16)$$

We use $\phi = \pi$ with various values of $\frac{d\phi}{dx}$ at $x = 0$, as our initial conditions throughout. We study this system for various values of N and ϵ . The solutions are characterized by the first integral of the static MSG equation, i.e.

$$P = -T_1^1 = \frac{1}{2} \left(\frac{d\phi}{dx} \right)^2 - V(\phi), \quad (17)$$

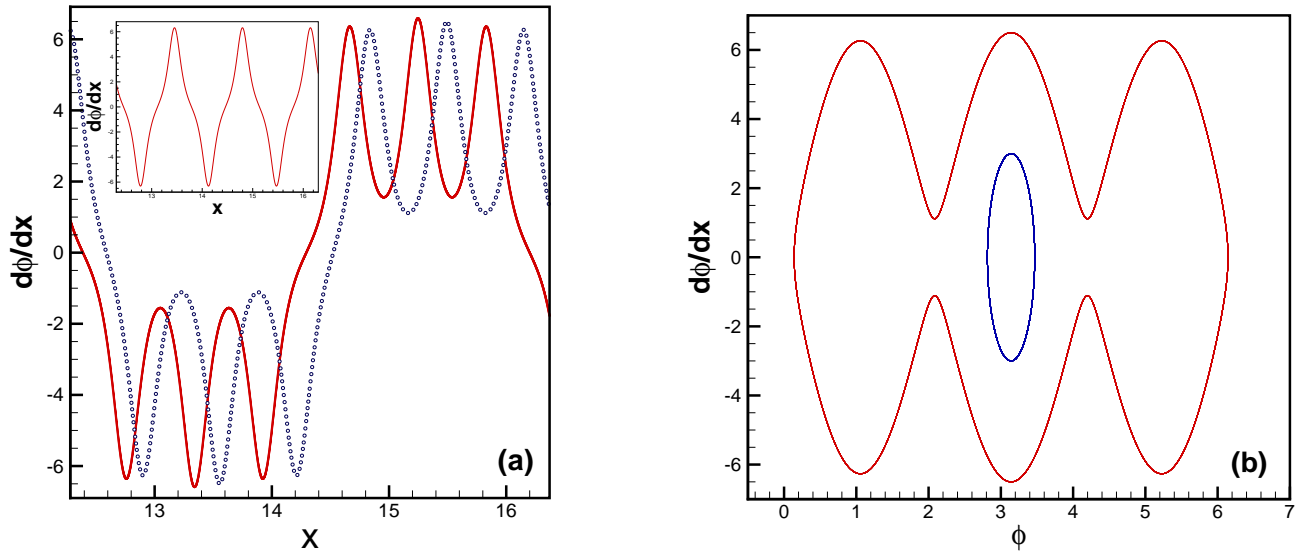


FIG. 3: (a) The slope diagram for the periodic chain of MSG solitons for $N = 3$ and $\epsilon = 10$, with $P = -0.2859$ for the solid curve and with $P = -0.8750$ dotted curve and $P = -2.0604$ for the inset. The three solutions have the same average density ($\bar{\rho}$) but different pressure (P). The main figure shows three subkink solutions while the inset shows a no-subkink solution. (b) The phase diagram ($\frac{d\phi}{dx}$ vs. ϕ) for the periodic chain of MSG solitons, for $N = 3$ and $\epsilon = 10$. The single loop corresponds to $P = -17.5$, (kink anti-kink), while the three lobe one corresponds to $P = -0.875$, (three subkinks).

with

$$\frac{dP}{dx} = 0. \quad (18)$$

Note that P is different from energy density

$$\rho = T_0^0 = \frac{1}{2} \left(\frac{d\phi}{dx} \right)^2 + V(\phi); \quad (19)$$

which changes with position x . The reason for using the letter P for this quantity is that it conforms with “pressure” for a one dimensional perfect fluid:

$$T_\nu^\mu = \text{diag}(\rho, -P). \quad (20)$$

Here, pressure is to be interpreted as tension, rather than force per unit area [1]. The value of P distinguishes two different type of solutions: (i) step-like solutions for which $P > 0$, which are the “running” solution of the mechanical analog, (ii) periodic solutions for which $-2(1 + \epsilon) < P < 0$, which are the “oscillatory” solutions of the mechanical analog[18]. Here, since we have chosen

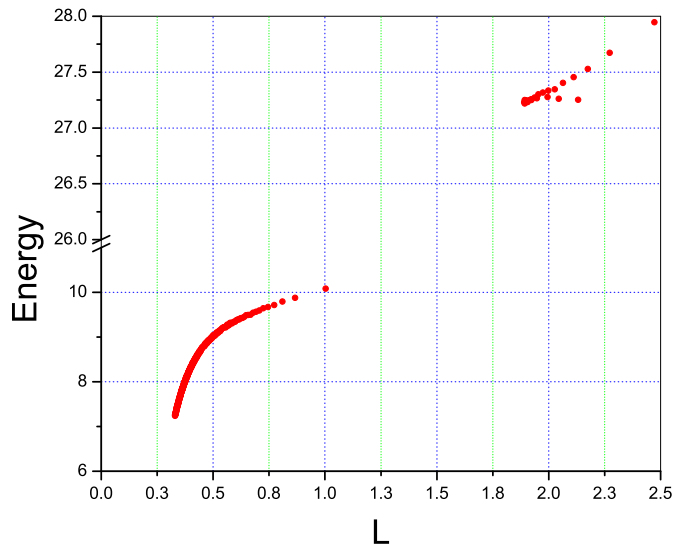


FIG. 4: Energy per soliton diagram for periodic chain of MSG solitons for $N = 3$ and $\epsilon = 10$. The low energy portion contains no subkinks while the high energy solitons is multi-valued and contains three-subkink solitons.

$\phi = \pi$ for all our solutions as an initial condition, the minimum value of P for periodic solutions is -2 for N even, where this lower bound is ϵ -dependent for odd N .

We first consider the simpler, step-like solutions. These solutions simply appear as in the case of DSG equations. The general MSG equation exhibits step-like solutions for $P > 0$ which are always characterized by N subkinks, as in Fig.2, provided that ϵ is in the appropriate range. However, as in the case of DSG equation, the periodic solutions exhibit a rich set of behavior depending on the value of P and ϵ , as well as N . A simple way to imagine these solutions is to consider slope diagrams ($\frac{d\phi}{dx}$ vs. x) or phase diagrams ($\frac{d\phi}{dx}$ vs. ϕ). Such a set is shown in Fig.3 for $N = 3$ and $\epsilon = 10$. We note that for $N = 3$, a kink anti-kink solution (with no subkinks) as well as a three-subkink solution is possible. Part(a) shows the kink anti-kink solution as an inset and two different three-subkinks in the main panel. Part (b) shows the phase diagram where each (subkink) solution is represented by a “loop” which is a helpful way of distinguishing these solutions.

A different (“thermodynamic”) method to characterize solutions of such systems is to consider the energy diagram (E vs. L) as well as equation of state diagram (P vs. $\bar{\rho}$)[1]. In the first case energy per soliton (E) is plotted as a function of inter-soliton distance (L)[19], while in the second case, P is plotted as a function of average energy density $\bar{\rho} = \frac{1}{l} \int_0^l \rho dx$ with l is a sufficiently large length (includes several solitons). These figures are shown for $N = 3$ and $\epsilon = 10$ in Fig.4 and

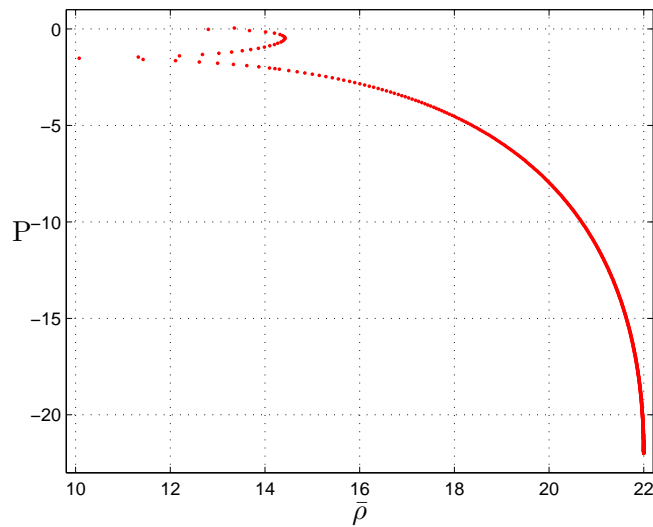


FIG. 5: Equation of state diagram for periodic chain of MSG solitons for $N = 3$ and $\epsilon = 10$. The upper curve corresponds to the three-subkink solutions and lower one to the no-subkink solutions.

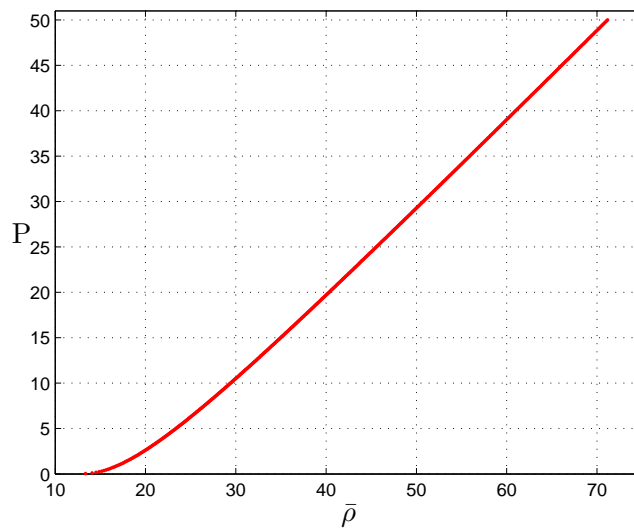


FIG. 6: The equation of state diagram for $N=3$, $\epsilon = 10$, for step-like solutions. The $P \rightarrow 0$ limit corresponds to the single kink solution. Unlike the periodic solutions, the general shape of this curve is independent of N .

Fig.5, respectively. As in the case with DSG equation, the energy diagram for $N = 3$ shows a region where E is double-valued. That is, Fig.4 shows a low energy solution with no subkinks, a region where no solutions are observed for our initial conditions, and a high energy region which is double valued. It is interesting to note that in the lower branch of high energy solution, as L

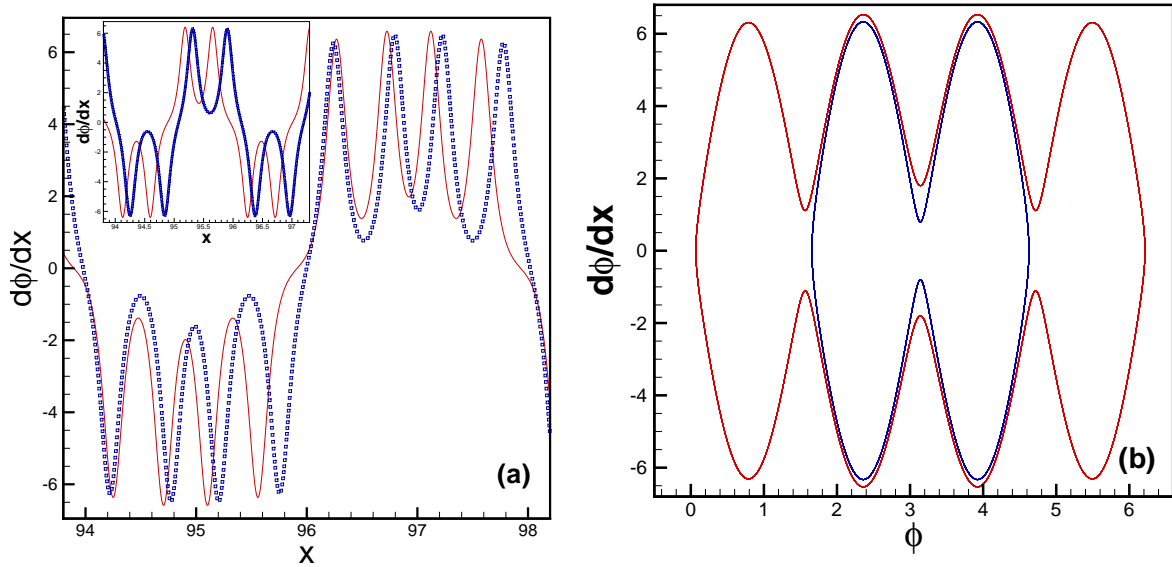


FIG. 7: (a) The slope diagram for the periodic chain of MSG solitons for $N = 4$ and $\epsilon = 10$, with $P = -0.0398$ for the solid curve and with $P = -0.70395$ dotted curve, with inset $P = -1.18080$ for the solid curve and $P = -1.8078$ dotted curve. The four solutions have the same average density ($\bar{\rho}$) but different pressure (P). The main figure shows four subkink solutions while the inset shows two subkink solutions. (b) The phase ($\frac{d\phi}{dx}$ vs. ϕ) diagram for the periodic chain of MSG solitons for $N = 4$ and $\epsilon = 10$. The two lobe loop corresponds to $P = -1.68$, while the four lobe one corresponds to $P = -0.38$.

increases, kink and anti-kink separate out, while in the upper branch it is the subkinks (within a given kink) which separate out when L increases. We note that in this three-subkink solution the middle subkink never changes and it is the other two (first and last) which actually extend out in the upper branch.

Fig.5 shows the equation of state for $N = 3$ and $\epsilon = 10$. It consists of two separate branches as well. The upper smaller branch is the three subkink solution and the lower longer branch is the no subkink solution. The upper branch is similar to that of DSG solution and the lower one is similar to the regular SG equation. The tension (or negative pressure) decreases in this 1d chain with increasing density due to the attractive force between the solitons in the chain. The only region where tension increases with increasing density is in the lower half of the upper branch which indicates a different type of inter-soliton force in the chain. It is worth noting that the equation of state diagram for the step-like solutions for $N > 2$ is in general no different than the $N \leq 2$ case previously studied [1]. Here we plot the $N = 3$ case in Fig.6.

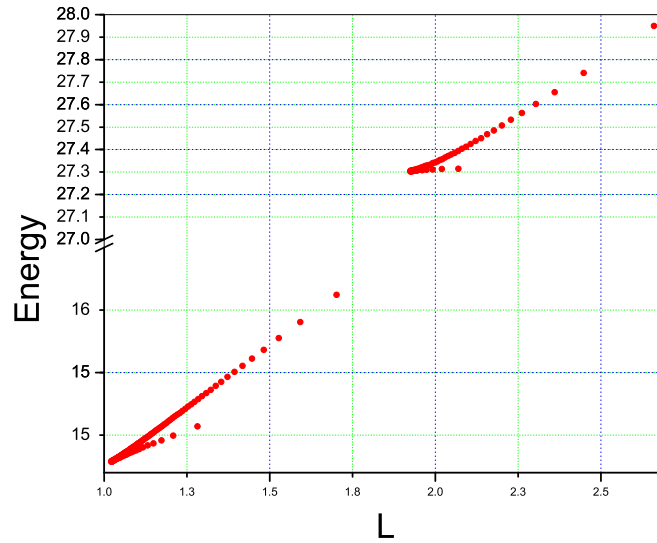


FIG. 8: Energy per soliton diagram for periodic chain of MSG solitons for $N = 4$ and $\epsilon = 10$. The upper curve corresponds to the four subkink solutions and the lower one to the two subkink solutions.

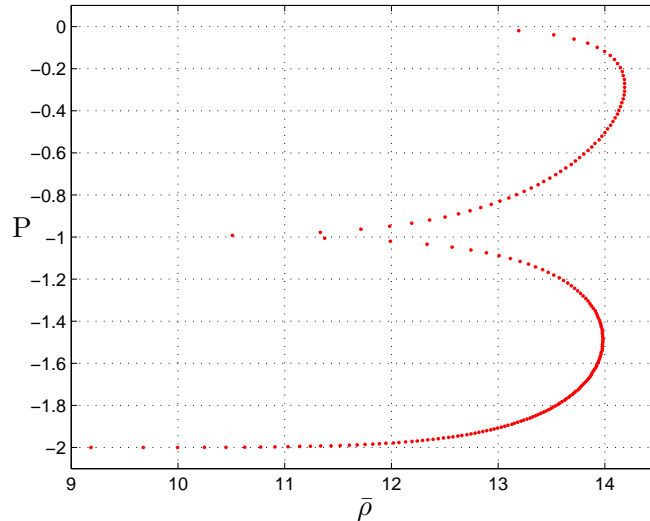


FIG. 9: The equation of state diagram for $N = 4$ and $\epsilon = 10$ system. The upper curve corresponds to the four subkink solutions and the lower one to the two subkink solutions.

IV. $N \geq 4$ CASES

As N increases, the MSG system gets more complicated and detailed. The main reason for this is the development of more subkinks. The emergence of subkinks in the periodic regime depends

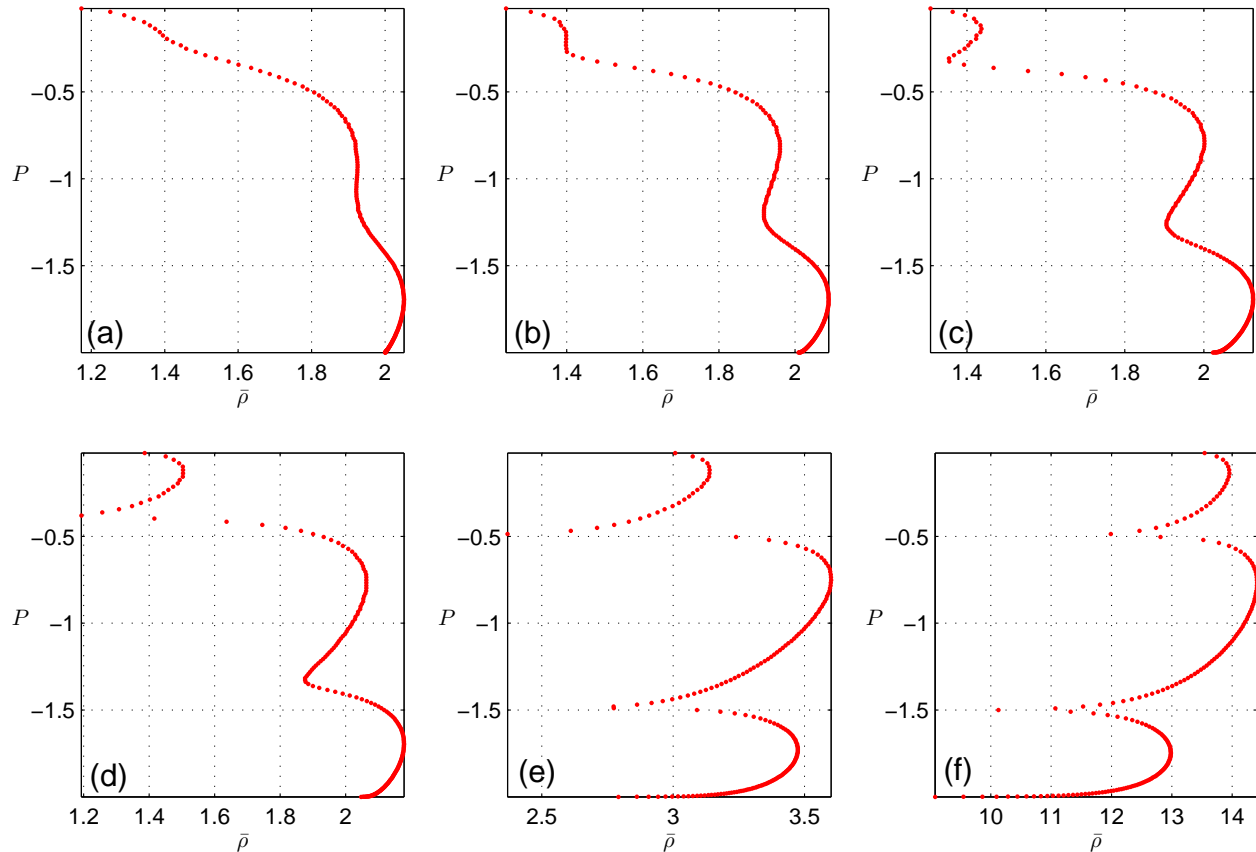


FIG. 10: The equation of state diagram for $N = 6$ and (a) $\epsilon = 0.03$, (b) $\epsilon = 0.05$, (c) $\epsilon = 0.07$, (d) $\epsilon = 0.1$, (e) $\epsilon = 1$ and (f) $\epsilon = 10$ system.

on the value of ϵ as well as P . The maximum number of possible subkinks is N . Due to the symmetry $V(\phi) = V(-\phi)$, the number of subkinks (n) is also “doubled”, i.e.

$$n = \begin{cases} 0, 2, 4, \dots \text{ up to } N & \text{for } N \text{ even} \\ 0, 3, 5, \dots \text{ up to } N & \text{for } N \text{ odd} \end{cases}$$

One can easily draw similar diagrams for general N as the ones drawn for $N = 3$ in the previous section. Here, we simply show these in Figs.7-9, for $N = 4$. Here, two and four subkink solutions are shown, with two subkink solutions being the low energy solutions and thus lower pressure.

The change in the equation of state diagram as ϵ increases shows an interesting behavior. This is shown in Fig.10 for $N = 6$. It is interesting to note how the multi-valuedness arises as ϵ is increased. As ϵ increases a larger range of $\bar{\rho}$ values allows multiple solutions. Another interesting behavior is

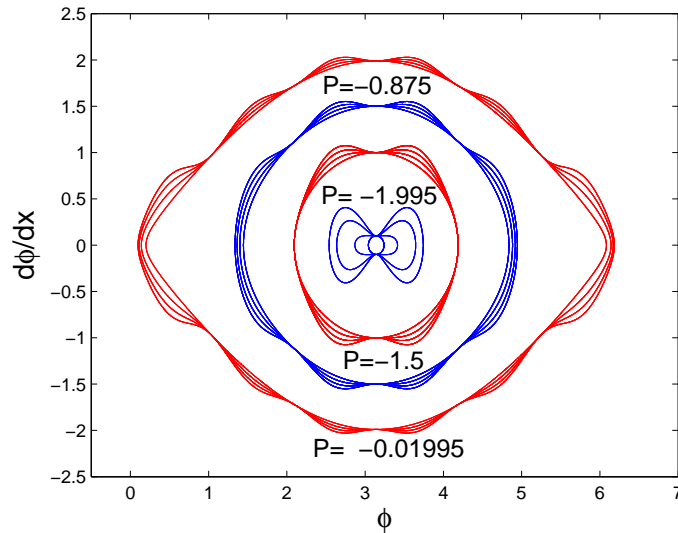


FIG. 11: The phase ($\frac{d\phi}{dx}$ vs. ϕ) diagram for the periodic chain of MSG solitons, for $N = 6$. The nearby curves correspond to $\epsilon = 0, 0.03, 0.06$ and 0.09 from the inner to the outer ones. The inner set of loops corresponds to $P = -1.995$, as indicated, all the way to $P = -0.01995$ for the other set of loops.

the emergence of cusp points with a discontinuity in $\frac{dP}{d\rho}$ (the left most section in Fig.10 (e) and (f)) which is due to the existence of hyperbolic unstable point in MSG equation. This discontinuity does not exist for the simple SG system. Note that these cusps separate regions of solutions with different number of subkinks. For example, in Fig.10(f) two cusps separate the 6, 4 and 2 subkink solutions. Another interesting point in these solutions is the maximum density solutions where compressibility ($\chi = \frac{d\rho}{dP}$) becomes zero. At these points the system becomes incompressible due to strong interactions of kink-antikink solutions (one can see that this corresponds to a minimum L)[1].

We are also interested to see how different subkink solutions arise as ϵ and P are changed. We therefore plot the phase diagram for various values of P and look for the emergence of subkinks as ϵ is increased. Such a plot for $N = 6$ is shown in Fig.11. Here, each set of loops corresponds to a given P value. It is seen that with a small change in ϵ subkink solutions arise. However, the number of subkinks is more sensitive to change in P than ϵ . We have observed that for a given value of P , increasing ϵ from zero can sometimes change the number of subkinks in a short interval. This interval is typically of order of $\epsilon \simeq 0.1$. After this brief transition, the number of subkinks remains constant. On the other hand the number of subkink changes with increasing P (for a given ϵ) until it reaches its maximum (N) for $P \rightarrow 0$.

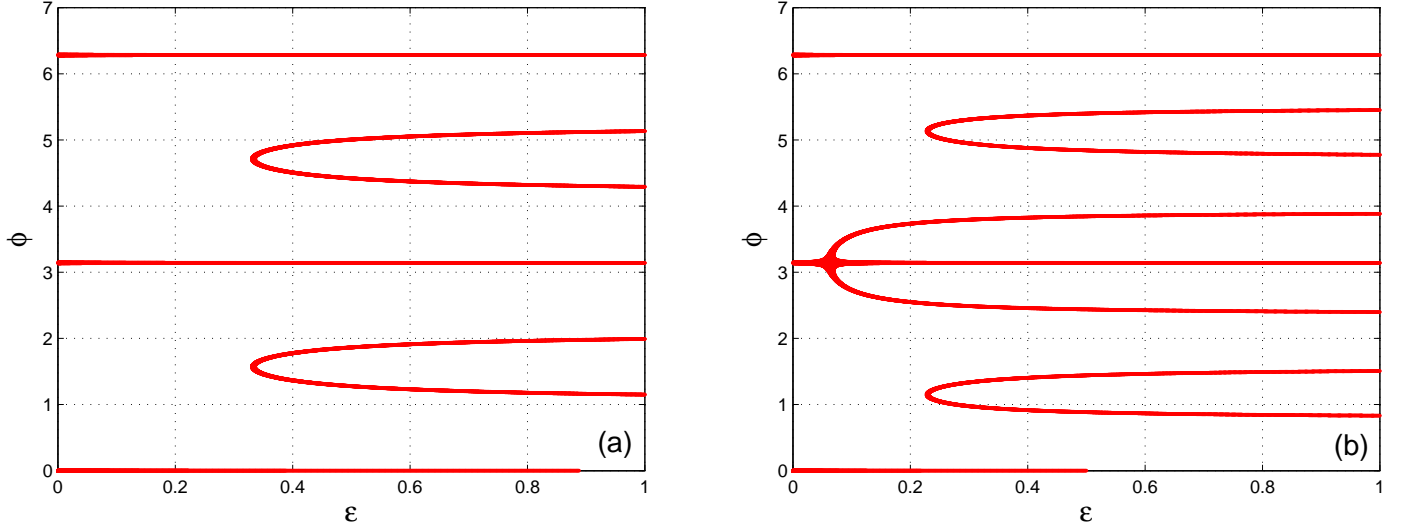


FIG. 12: Fixed points of the MSG equation for (a) $N = 3$ and (b) $N = 4$.

V. STABILITY AROUND FIXED POINTS

The fixed points of the MSG equation are obtained by equating the RHS of the equation (3) to zero:

$$\sin \phi + N\epsilon \sin(N\phi) = 0. \quad (21)$$

Let us call these fixed points which lie in the range $[0, 2\pi]$ as $\phi_n (n = 1, 2, \dots)$. The number of fixed points depends on both values of N and ϵ . Fig.12 shows the value and number of fixed points as ϵ varies for two cases of $N = 3$ (Fig.12a) and $N = 4$ (Fig.12b).

In order to investigate the stability of periodic solutions around fixed points, we use the conventional linear perturbation analysis, by inserting the expression

$$\phi(x, t) = \phi_n + A \cos(kx) \cos(\omega t), \quad (22)$$

in which $A (\ll \phi_n)$ is a constant and k and ω are wave number and angular frequency, respectively, in to the field equation (3). Expanding the nonlinear sine terms and keeping only terms linear in A , we obtain

$$\omega^2 = k^2 + \cos \phi_n + N^2 \epsilon \cos(N\phi_n); \quad (23)$$

In this dispersion relation, the stability is judged by the sign of ω^2 for any chosen value of k . Let us write Eq.(23) in the form

$$\omega^2 = k^2 + f_n(N, \epsilon). \quad (24)$$

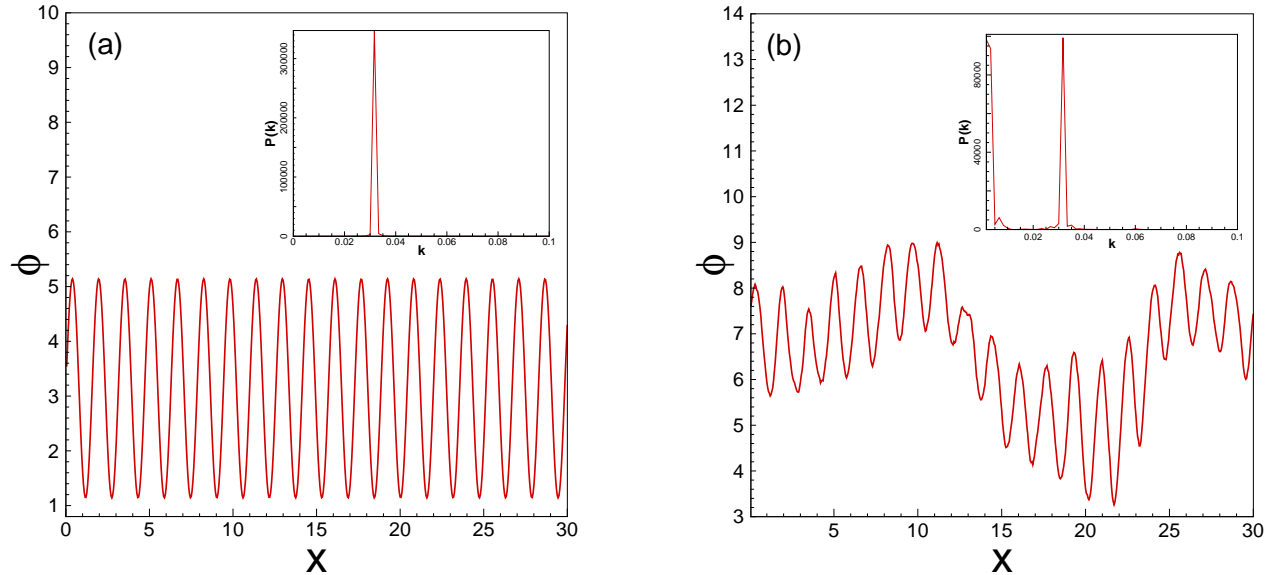


FIG. 13: (a) Initial periodic perturbation around the fixed point of DSG ($\phi = \pi$) for $\epsilon = 0.1$ and its FFT(inset), (b) The evolved perturbation after 200 time steps and the corresponding FFT.

It is obvious that if $f_n > 0$, ω^2 is always greater than zero and the perturbation is stable. If, on the other hand, $f_n < 0$, ω^2 is positive and we have stability, only for $k^2 > -f_n$ or $\lambda < \frac{2\pi}{\sqrt{-f_n}}$. In such a case, we expect small scale perturbations to be stable and long ones to be unstable. The fore-mentioned linear analysis was checked numerically, by using a finite difference algorithm[17]. We have performed numerical experiments with periodic perturbations around a fixed point as initial condition. In this way, we could confirm stability about the minima-energy fixed points like $\phi_n = 0$. Perturbations around local maxima show a more interesting behavior. It was seen that short wavelength modes remain stable, while long wavelength ones start to be excited and increase in amplitude. Fig.13 shows the fate of a periodic perturbation around $\phi_n = \pi$ in the DSG system ($N = 2$). The initial perturbation is shown in Fig.13a together with its FFT. Fig.13b shows the perturbation after integrating the dynamical equation for 200 time steps. As the FFT shows, the initial, small wavelength perturbation persists, while the unstable, long wavelength modes grow, confirming our analytical result.

VI. CONCLUDING REMARKS

We have examined the periodic and step-like solutions of the MSG system. In particular, we interpreted the step-like and periodic solutions as a many body system of kinks and anti-kinks with a nonlinear interaction between the solitons. This interpretation is established by comparing the asymptotic $P \rightarrow 0$ case with the single-soliton solution. In this limit, each site in the chain conforms with the single-soliton solution, and the energy per soliton approaches the single-soliton energy. As the solitons get closer, the energy per soliton becomes different and the difference is attributed to the interaction energy.

We observed that as N increases, more and more subkinks (up to N) can develop and this leads to a more complicated equation of state. This diagram becomes multiple-valued, depending on the number of subkinks, which in turn depends on the pressure P . We examined the stability of periodic solutions around the fixed point ($\phi = \pi$ and $\frac{d\phi}{dx} = 0$), obtaining the interesting result that within the linear approximation, short wavelength periodic solutions oscillate like standing waves (signalling stability), while long wavelength periodic solutions are unstable.

-
- [1] M. Peyravi, A. Montakhab, N. Riazi and A. Gharaati, Eur. Phys. J. **B 72**, 269-277 (2009).
 - [2] S. Burdick, M.El-Batanouny and C. R. Willis, Phys. Rev. **B 34**, 6575 (1986).
 - [3] K. Maki and P. Kumer, Phys. Rev. **B 14**, 118 (1976); **14**, 3290 (1976).
 - [4] Y. Shiefman and P. Kumer, Phys. Scr. **20**, 435 (1979).
 - [5] K. M. Leung, Phys. Rev. **B 27**, 2877 (1983).
 - [6] O. Hudak, J. Phys. Chem. **16**, 2641 (1983); **16**, 2659 (1983).
 - [7] M. El-Batanouny, S. Burdick, K. M. Martini and P. Stancioff, Phys. Rev. Lett. **58**, 2762 (1987).
 - [8] E. Magyari, Phys. Rev. **B 29**, 7082 (1984).
 - [9] J. Pouget and G. A. Maugin, Phys. Rev. **B 30**, 5306 (1984); **31**, 4633(1984).
 - [10] N. Hatakenaka, H. Takayanagi, Y.Kasai and S. Tanda, Physica **B 284-288** (2000) 563-564.
 - [11] T. Uchiyama, Phys. Rev. **D 14**, 3520 (1976).
 - [12] S. Duckworth, R. K. Bullough, P. J. Caudrey and J. D. Gibbon, Phys. Lett. **57 A**, 19 (1976).
 - [13] V. A. Gani and A. E. Kudryavtsev, Phys. Rev. **E 60**, 3305 - 3309 (1999).
 - [14] M. Croitoru, J. Phys. A: Math. Gen. **22**, 845-863 (1989).
 - [15] C. A. Popov, Wave Motion. **42(1)**, 309-350 (2006).
 - [16] N. Riazi and A. R. Gharaati, Int. J. Theor. Phys. **37**, 1081 (1998).
 - [17] E. Kreyszig, *Advanced Engineering Mathematics*, John Wiley and Sons, NewYork(1983).
 - [18] This problem has a simple mechanical analog if the following change of variables are considered $x \rightarrow t$,

$\phi \rightarrow x$, for a particle of unit mass.

[19] Here, we use the word soliton interchangeably with kink. The distance between successive kinks (L) is well-defined, and therefore energy per soliton (E) is well-defined as well.